The Late Miocene climate response to a modern Sahara desert

Arne Micheels [a,*], Jussi Eronen [b], Volker Mosbrugger [a]

[a] *Senckenberg Research Institute and Natural History Museum, Biodiversity and Climate Research Centre (LOEWE BiK-F), Senckenberganlage 25, D-60325 Frankfurt/Main, Germany*
[b] *Department of Geology, P.O. Box 64, FIN-00014 University of Helsinki, Finland*

ARTICLE INFO

ABSTRACT

The climate cooling and vegetation changes in the Miocene/Pliocene are generally well documented by various proxy data. Some important ecosystem changes occurred at that time. Palaeobotanical evidence suggests that the Sahara desert first appeared in the Pliocene, whereas in the Miocene North Africa was green. In the present study, we investigate the Late Miocene climate response to the appearance of the Sahara desert from a climate modelling sensitivity experiment. We compare a model experiment, which includes a full set of Late Miocene boundary conditions, with another one using the same boundary conditions except that the North African vegetation refers to the present-day situation. Our sensitivity study demonstrates that the introduction of the Sahara desert leads to a cooling and an aridification in Africa. In addition, we observe teleconnection patterns related to the North African desertification at around the Miocene/Pliocene boundary. From our sensitivity experiment, we observe that the Sahara contributes to a cooling in Central Asia and in North America. As compared to hypsodonty data for Central Asia, an increased aridity is underestimated in the Sahara experiment. Finally, we observe that the introduction of the Sahara leads to a cooling in the northern high latitudes. Hence, our sensitivity experiment indicates that the appearance of the Sahara desert is one piece to better understand Late Cenozoic climate cooling being most pronounced in the high latitudes.

1. Introduction

During the Cenozoic, the climate successively changed from the warm-humid greenhouse climate of the Paleogene into the Quaternary icehouse phase characterised by its glacial–interglacial cycles (e.g., Retallack, 2001; Zachos et al., 2001). The Miocene belongs to the late phase of the Cenozoic cooling. The Miocene was still warmer and more humid than today (e.g., Wolfe, 1994a,b; Bruch et al., 2004; Jimenez-Moreno et al., 2005; Mosbrugger et al., 2005), but towards the Pliocene it changed into the modern situation (Fauquette et al., 2007). The late Cenozoic climate cooling was most pronounced in higher latitudes. Corresponding to the overall climate transition in the Cenozoic, vegetation underwent relevant changes (e.g., Jacobs et al., 1999; Willis and McElwain, 2002; Jacobs, 2004; Mosbrugger et al., 2005). First grasslands appeared in the Eocene, but they were no major ecosystems until the Oligocene or even later (e.g., Pott, 1995; Retallack, 2001; Jacobs, 2004). Palaeobotanical data indicate significant vegetation changes from the Early to the Late Miocene (e.g., Wolfe, 1985; Strömberg, 2002; Willis and McElwain, 2002; Strömberg, 2004; Mosbrugger et al., 2005). In the Early Miocene, North Africa was dominated by tropical trees (e.g., Wolfe, 1985; Dutton and Barron, 1997; Jacobs, 2004) and vegetation cover changed into a more open grassland vegetation towards the end of the Miocene (e.g., Cerling et al., 1997a,b; Pickford, 2000; Jacobs, 2004).

Africa became more arid during the latest Miocene and early Pliocene (e.g., Cerling et al., 1997a; Jacobs et al., 1999; Jacobs, 2004; Behrensmeyer, 2006). At around the Miocene/Pliocene boundary, the Sahara desert appeared for the first time (e.g., Le Houerou, 1997; Pickford, 2000; Vignaud et al., 2002; Willis and McElwain, 2002; Schuster et al., 2006). Evidences from the Central Sahara suggest the presence of desert since ~7 Ma (e.g., Vignaud et al., 2002; Schuster et al., 2006).

Based on well-documented evidences from the fossil record, several climate modelling studies analysed the processes behind the Cenozoic cooling, but the role of vegetation has attracted relatively little interest so far. Palaeoclimate model experiments primarily focused on the role of mountain uplift or the effects of a different-than-present palaeogeography in the Miocene (Ramstein et al., 1997; Ruddiman et al., 1997; Fluteau et al., 1999; Liu and Yin, 2002; Kutzbach and Behling, 2004; Sepulchre et al., 2006; Steppuhn et al., 2006). For instance, the uplift of the Tibetan Plateau contributed to an intensification of the Asian monsoon from the Oligocene to today (Fluteau et al., 1999; Liu and Yin, 2002). In particular, Liu and Yin (2002) demonstrated that Tibet uplift not only intensifies the monsoon system, but also affects North Africa. The uplift of Tibet leads to a decrease of soil moisture in North Africa (Liu and Yin, 2002). If so, it is likely to assume that the aridification of North Africa in the Miocene/Pliocene (cf. above) can have been related to Tibet uplift, but this hypothesis has not yet been tested with climate model experiments. Vegetation changes in Africa from the Miocene to the Pliocene are also directly linked to the East African Rift system because tectonic uplift in that region causes increased aridity in North Africa

* Corresponding author.
E-mail address: arne.micheels@senckenberg.de (A. Micheels).

(Sepulchre et al., 2006). External factors such as mountain uplift, atmospheric CO_2 and orbital forcing triggered the climate and, thus, initiated the onset of the North African aridification. However, warm polar regions in the Miocene and the high-latitude cooling during the late Cenozoic are not sufficiently understood (e.g., Steppuhn et al., 2006, 2007; Micheels et al., 2007).

The appearance of the Sahara desert at around the Miocene/Pliocene boundary was not the cause for the overall late Cenozoic climate cooling. However, no climate modelling experiment yet focused specifically on the global climate response to the North African vegetation change in the Miocene/Pliocene. On the global scale, Dutton and Barron (1997) investigated the climatic effects of the Early Miocene vegetation, which is primarily characterised by a larger-than-present forest cover. As compared to an Early Miocene model experiment with modern vegetation, the study pointed out that the palaeovegetation generally contributed to warmer polar conditions in the Early Miocene than today. For the Middle Pliocene, Haywood and Valdes (2006) analysed the coupled climate–vegetation system showing a global trend towards a larger forest cover in the Pliocene and a reduced Sahara desert as compared to today. If, however, the Early Miocene and the Mid-Pliocene vegetation are globally so much different from the modern one, it is not possible to identify climate patterns (e.g., teleconnections), which can be attributed to a specific region. Quaternary model experiments focused on the climatic changes due to a different vegetation cover in North Africa during the Last Glacial Maximum, in the mid-Holocene, and today (e.g., Claussen and Gayler, 1997; Brovkin et al., 2002). On the one hand, even a greener North Africa in the mid-Holocene still represents some deserted areas (Brovkin et al., 2002), which is different to the Miocene/Pliocene situation. On the other hand, it was emphasised that the understanding of climate–vegetation processes from Quaternary model simulations cannot easily be transferred to the future climate change (Claussen et al., 2003). Therefore, the general Quaternary ice-house is also not necessarily an analogue for pre-Quaternary greenhouse phases such as the Miocene/Pliocene.

So far, the understanding of the global climate cooling from the Miocene to present is not complete. In particular, the question about what climate changes are related to regional vegetation changes such as the North African desertification in the Neogene remains insufficiently open. Aiming to better understand the Miocene-to-present cooling, we perform a climate modelling sensitivity experiment with an Earth system model of intermediate complexity (EMIC), where we test the climate response to the introduction of the Sahara desert in the late Neogene. As compared to highly complex models, EMICs are generally simpler, but computationally much more efficient. In terms of model experiments, relatively little work has been done for the Miocene. In fact, there is a need for the use of highly complex even coupled atmosphere–ocean models, but EMICs are efficient tools for some fundamental sensitivity studies like our present study. We concentrate more on the global-scale climate response to the appearance of the Sahara desert and present a modelling study, which integrates the fossil record: We validate the consistency of climate patterns of our model experiment with climate proxy data obtained from mammalian fossils as well as we consider climate information available from other studies. Therewith, the sensitivity experiment can contribute to interpret climate changes/variability documented in the fossil record as well as the model validation helps to assess the reliability of the model results due to several uncertainties in the model physics and its boundary conditions. The combined climate modelling-proxy data study contributes to better understand the general late Cenozoic cooling trend. The intention of the present sensitivity experiment is to understand the direct effects (e.g., albedo effect) of a regional vegetation change in North Africa in the Miocene and the related teleconnection patterns; i.e. we consider only the effects of vegetation on climate and exclude climate–vegetation-interaction processes. Based on our approach with a prescribed regional vegetation change, further climate modelling experiments using dynamic vegetation modules can focus on feedback mechanisms, which amplify or dampen signals of direct effects. Our approach of not using a dynamic vegetation module is also motivated by the fact that feedback mechanisms can depend on (uncertainties of) boundary conditions. Hence, our present study is a first step to understand climatic effects of regional vegetation changes in the Late Miocene.

2. Model description and experimental design

Analysing the climate response to the introduction of the Sahara desert in North Africa in the Late Neogene, we use the Earth system model of intermediate complexity Planet Simulator (Fraedrich et al., 2005a,b) developed at the Meteorological Institute of the University of Hamburg (http://www.mi.uni-hamburg.de/downloads-and-related-papers.245.0.html). The spectral atmospheric general circulation model (AGCM) PUMA-2 is the core module of the Planet Simulator. The resolution of the model is T21 ($5.6° \times 5.6°$) with 10 vertical layers using terrain-following σ-coordinates. The atmosphere model is an advanced version (e.g., including moisture in the atmosphere) of the simple AGCM PUMA (Fraedrich et al., 1998; Frisius et al., 1998). As compared to the first 'dry-dynamics version', the atmosphere module was upgraded with schemes for various physical processes such as radiation transfer, large-scale and convective precipitation, and cloud formation. In the Planet Simulator, the atmosphere is coupled to a slab ocean and a thermodynamic sea ice model. Both modules can either use a flux correction to realistically represent the heat exchange with the atmosphere or prescribed sea surface temperatures (SSTs) and sea ice. The Planet Simulator also includes a land surface module. Amongst others, simple bucket models parameterise soil hydrology and vegetation. As compared to highly complex general circulation models, the EMIC conception of the Planet Simulator is relatively simple, but the model proved its reliability. The Planet Simulator was repeatedly used for present-day climate modelling experiments (e.g., Fraedrich et al., 2005b; Junge et al., 2005; Grosfeld et al., 2007; Kleidon et al., 2007) and for past climates (Micheels et al., 2006; Romanova et al., 2006; Micheels and Montenari, 2008). For the Late Miocene, Micheels et al. (2006, submitted for publication) presented that the Planet Simulator is consistent to previous Late Miocene model experiments (Micheels et al., 2007) with a complex AGCM. For a more complete model description, we refer the reader to the documentation of the Planet Simulator (Fraedrich et al., 2005a,b).

As a reference base of our sensitivity experiment, we use a Late Miocene (Tortonian, 11 to 7 Ma) model experiment. In the following, this experiment is referred to as TORT. In principle, boundary conditions of TORT are based on Late Miocene simulations with the highly complex AGCM ECHAM4 coupled to a mixed-layer ocean model (Steppuhn et al., 2006; Micheels et al., 2007). Due to the coarse model resolution, the Late Miocene land–sea-distribution in TORT (included in Fig. 2) is equal to the modern one, but we include the Paratethys (after Popov et al., 2004). The palaeorography is generally lower than present in TORT (Steppuhn et al., 2006; Micheels et al., 2007). For instance, the Tibetan Plateau reaches half of its present elevation. In fact, the southern part, the Himalayas, could have been as high as today since the Middle Miocene (Spicer et al., 2003), but the overall elevation of the Tibetan Plateau in the Miocene was lower than present (e.g., Molnar, 2005). The palaeovegetation also refers to the Tortonian (Micheels et al., 2007) and represents a generally larger forest cover than today. In particular, boreal forests extend far towards northern high latitudes. Deserts/semi-deserts and grasslands are reduced as compared to nowadays. Atmospheric CO_2 is set to 280 ppm in the Tortonian reference simulation. This value does not only correspond to the pre-industrial level, but it is also reasonable for the Late Miocene (Pearson and Palmer, 2000; Pagani et al., 2005), although it could have been at present-day level or even higher (e.g., Kürschner et al., 1996; MacFadden, 2005). The ocean is initialised using 'palaeo-SSTs' from a previous Tortonian run (Micheels et al., 2007). Northern Hemisphere's sea ice is initially removed. After the initialisation with palaeo-SSTs, we continue the model integration

using the slab ocean with a present-day flux correction. It is commonly known that the northward ocean heat transport in the Miocene was relatively weak as compared to today (e.g., Bice et al., 2000; Steppuhn et al., 2006), whereas it was stronger-than-present in the Pliocene (e.g., Haywood et al., 2000a,b). Hence, the choice of the present-day flux correction for our experiments best represents the situation in between.

Based on TORT, we define our vegetation sensitivity scenario, which is referred to as SAHARA in the following. For SAHARA, we introduce the modern Sahara desert in North Africa, i.e. we replace the Tortonian grassland to savannah vegetation with the modern Sahara desert (e.g., Fig. 2 illustrates the modified area). This may not be fully realistic for the Miocene/Pliocene situation (e.g., Schuster et al., 2006), but the extent of the Sahara was possibly large. Even if we overestimate the size of the Sahara desert, this setting allows us to estimate a maximum atmospheric response to the North African desertification. All other boundary conditions in SAHARA remain the same as in TORT. For both experiments, we perform integrations over 200 years and we consider the last 10 simulation years for our data analysis. The difference between both runs, SAHARA minus TORT, represents the climate response to the introduction of the Sahara
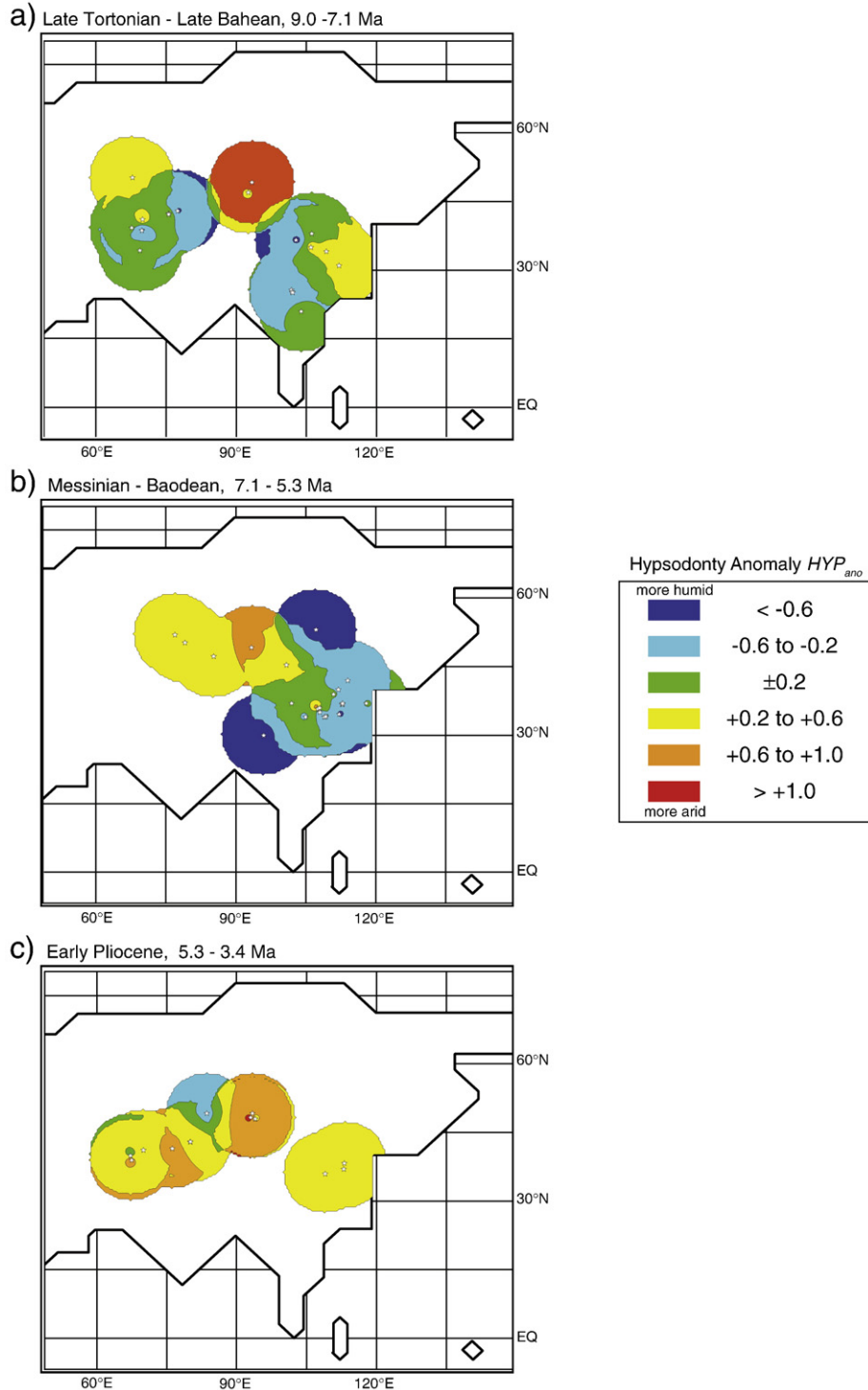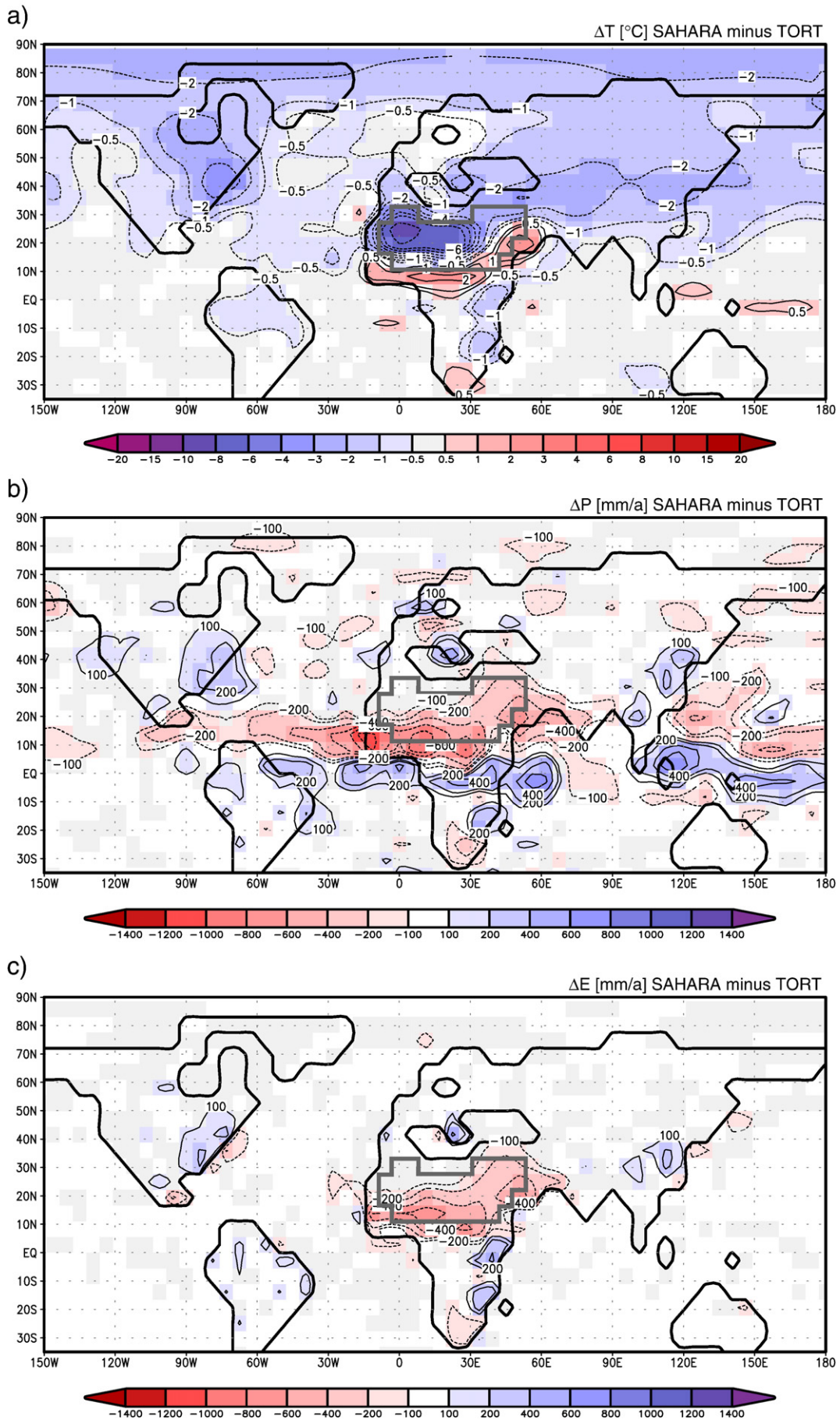

Fig. 1. The large mammal hypsodonty anomalies for Asia in a) the late Tortonian, b) the Messinian, and c) the Early Pliocene. Positive/negative anomalies indicate more arid/humid conditions with respect to the average. For mapping, values were interpolated with a cell size of 50 km, a search radius of 1000 km and a grid border of 1000 km.
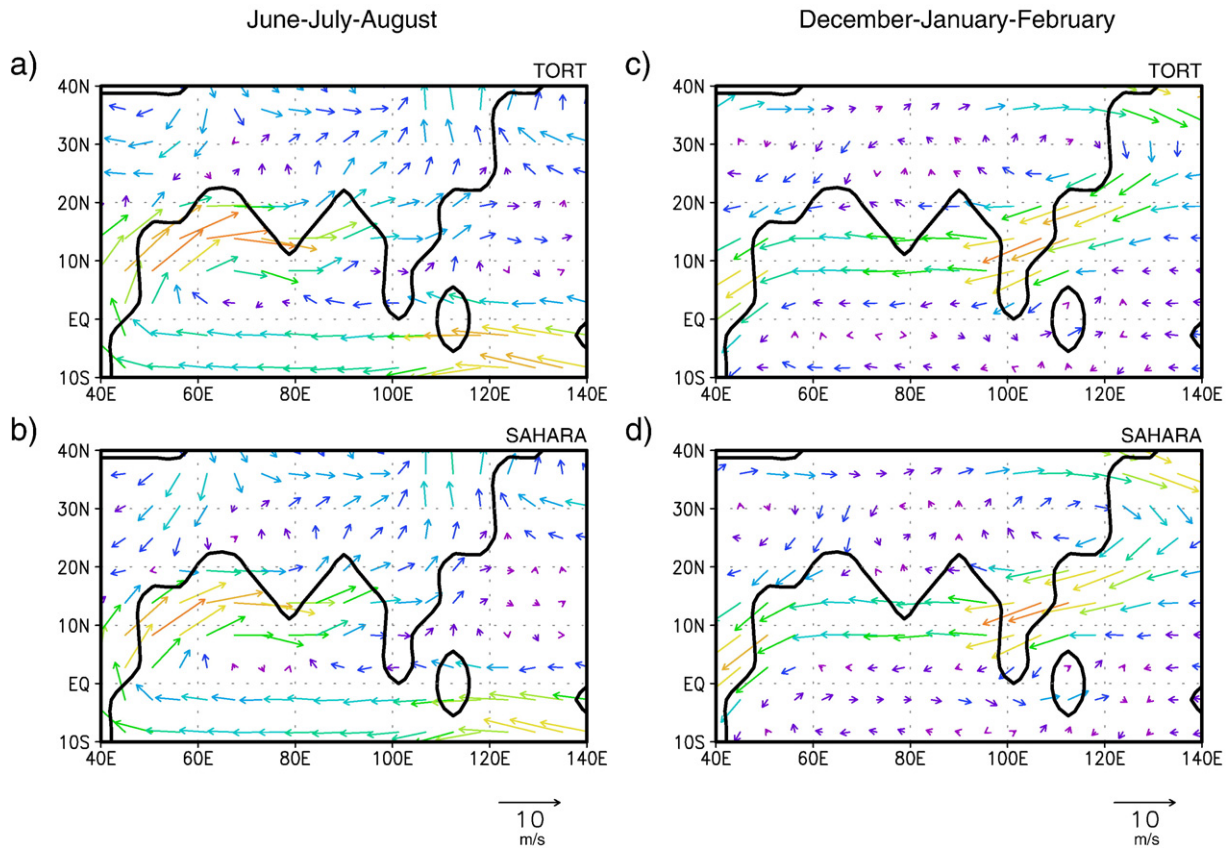
a)

ΔT [°C] SAHARA minus TORT

b)

ΔP [mm/a] SAHARA minus TORT

c)

ΔE [mm/a] SAHARA minus TORT

June-July-August   December-January-February

Fig. 3. The horizontal wind field (m/s) at 850 hPa for Asia of a) TORT and b) SAHARA in June–July–August, and c) and d) in December–January–February. The reference arrow represents 10 m/s.

desert in the Late Miocene. It should be noted that in the real world vegetation changes themselves are a response to climatic changes, which then feedback to climate again. Only in our model domain, the Sahara desert is the cause of climate changes (and not necessarily the resulting climate situation is able to maintain the introduced vegetation change).

3. Large mammal hypsodonty

In order to appropriately validate our model results, we use large mammal hypsodonty (tooth crown height) from the NOW-database (http://www.helsinki.fi/science/now) as proxy data. The stratigraphy of the NOW database is based on Steininger et al. (1996) and Steininger (1999). In addition, we use the biochronology established by Zhang and Liu (2005) for Chinese mammal localities. Following these authors, the Chinese faunal unit Bahean correlates with the Tortonian in Europe and the Baeodean is the pendant of the Messinian. We consider only herbivorous large mammals, while small mammals (orders Insectivora, Chiroptera, Rodentia, Lagomorpha) and carnivores (orders Carnivora and Creodonta) are not taken into account. In addition, we just use localities with at least two ordained hypsodonty scores. Showing the environmental development according to large mammal record, we use their tooth crown height to estimate annual rainfall (Fortelius et al., 2002). Generally, hypsodonty is regarded as an adaptation to increased water stress (i.e., aridity). There is a fuzzy, but statistically highly significant relationship between mean annual precipitation and the mean hypsodonty of modern large mammal communities (Damuth and Fortelius, 2001). Even though the method

has some limitations, it already proved its reliability to estimate annual precipitation in Eurasia for several Neogene time intervals (Fortelius et al., 2002, 2003; Eronen and Rook, 2004; Fortelius et al., 2006). Hypsodonty raw data were generally processed as described in detail in Fortelius et al. (2002). For the maps shown in the following (Fig. 1), we calculated the mean hypsodonty from all data of the three time intervals ($\overline{HYP} = 1.7$) and define hypsodonty anomalies as deviations from the average ($HYP_{ano} = HYP - \overline{HYP}$).

4. Results

On the global scale, the Tortonian reference run has an average temperature of 16.0 °C. This is $+2.6$ °C warmer than a present-day control experiment (13.4 °C) with the Planet Simulator using the same set of boundary conditions as the complex AGCM ECHAM5 (e.g., Roeckner et al., 2006) and a pCO_2 of 360 ppm. In our Sahara simulation, the global temperature (15.3 °C) is slightly lower than in TORT (-0.7 °C). The global precipitation in SAHARA (1067 mm/a) tends to represent drier (-19 mm/a) conditions than the Tortonian reference run (1086 mm/a). Consistent to the cooling trend in SAHARA, the global sea ice cover increases ($+12\%$) as compared to TORT.

Fig. 2 illustrates mean annual temperature and precipitation differences between SAHARA and TORT. The introduction of the Sahara desert leads to a significant cooling of partly more than -8 °C in North Africa (Fig. 2a), which is due to the higher albedo of desert as compared to the grassland vegetation in TORT. Annual rainfall decreases by more than -1000 mm/a in Central Africa as compared to TORT (Fig. 2b), whereas the most northern part of Africa is not noticeably drier in the

Fig. 2. a) The annual average temperature differences (°C), b) the annual average precipitation rate differences (mm/a), and c) the annual average evaporation rate differences (mm/a) between SAHARA and TORT. Non-coloured white areas represent non-significant differences with a Student's t-test ($p = 0.05$). The grey line illustrates the area of the modern Sahara desert. (For interpretation of the references to colour in this figure legend, the reader is referred to the web version of this article.)

Sahara run. In contrast to the north, the part south of the modified area in North Africa gets warmer (+2 °C) in SAHARA (Fig. 2a), which is linked to strongly decreased rainfall (Fig. 2b) as compared to TORT. Precipitation in this area is reduced because of a lower evaporation (Fig. 2c) in the Sahara experiment. Correspondingly, evaporative cooling is reduced as compared to TORT. This leads to a warming, which dominates over the cooling due to the albedo effect. Hence, the more northern part of the Sahara responds more to the increased albedo in SAHARA as it is already an arid region in TORT. Contrarily, the more humid southern area reacts more sensitive on evaporative cooling in our experiments.

In the Sahara simulation, Asia is significantly cooler than in TORT (Fig. 2a). The cooling in SAHARA is most pronounced (−2 °C) from Iran to the Tibetan Plateau and in northern China. This indicates that the appearance of the Sahara desert contributes to a cooling trend in Asia. From Turkey to India, the precipitation (Fig. 2b) is significantly lower than in TORT, indicating that the Indian summer monsoon is weaker in SAHARA (Fig. 3). Precipitation in N- and NE-Asia does not change much in SAHARA (Fig. 2b), but it represents a trend towards drier conditions than in TORT. E-/SE-Asia tends to be more humid (+200 mm/a) than TORT. This describes a weak intensification of the SE-Asian monsoon in SAHARA, which is pronounced during the winter season (Fig. 3).

Focusing on the mid- and high latitudes, the Sahara experiment is generally cooler than TORT (Fig. 2a). In North America, the North African desertification causes a cooling of −2 °C to −4 °C. Along the eastern coast of N-America, precipitation increases by up to +200 mm/a
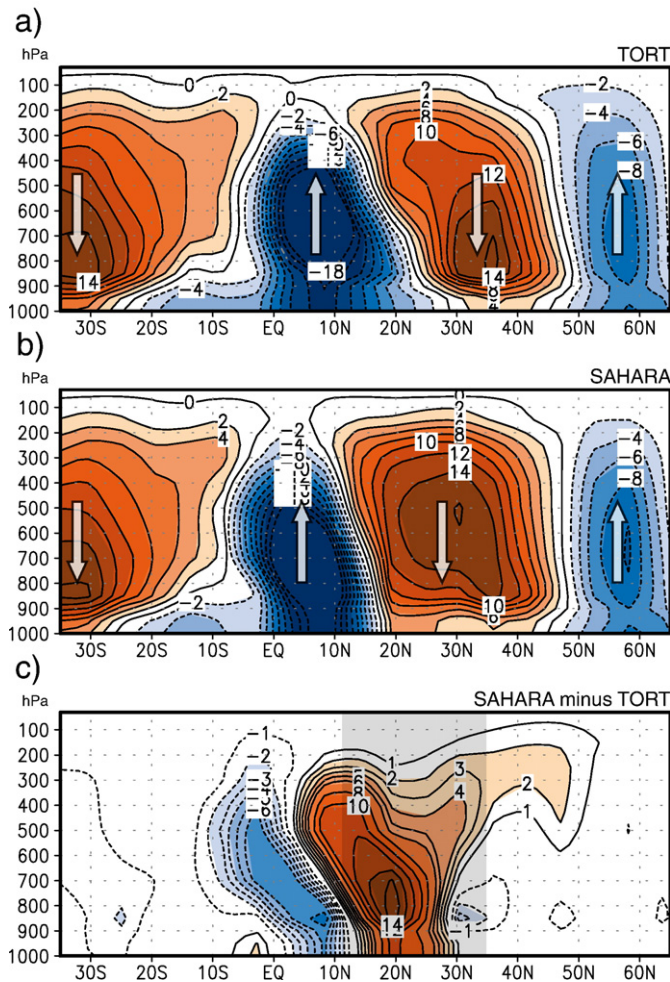

Fig. 4. The zonal average of the vertical wind (×10³ Pa/s) for North Africa (25°W to 60°E, 35°S to 65°N) of a) TORT, b) SAHARA, and c) the differences between SAHARA and TORT. The grey-shading in c) illustrates the position of the modern Sahara desert. (For interpretation of the references to colour in this figure legend, the reader is referred to the web version of this article.)
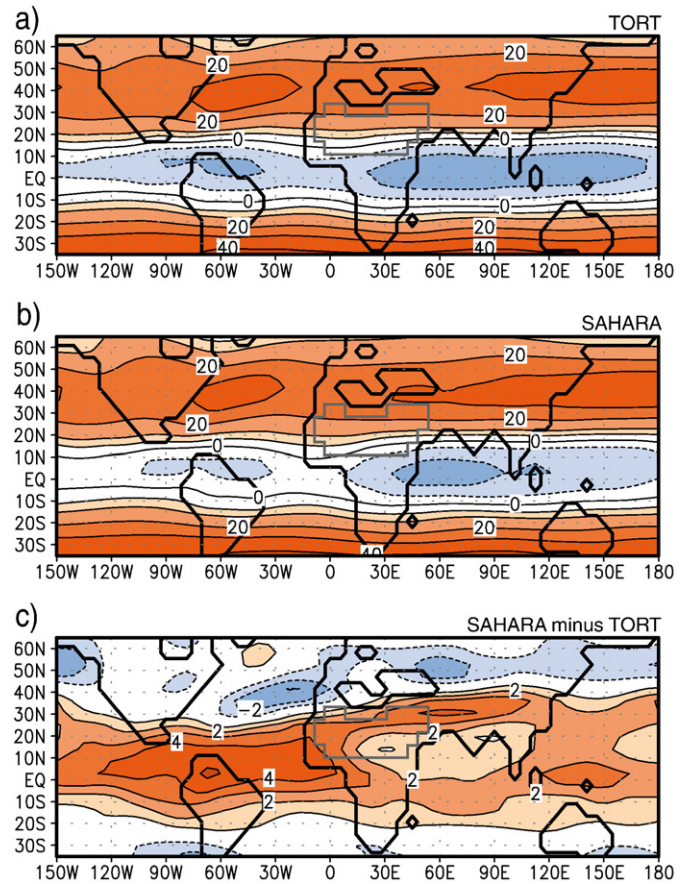

Fig. 5. The annual average zonal wind (m/s) at 200 hPa of a) TORT, b) SAHARA, and c) the differences between SAHARA and TORT. The grey line illustrates the area of the modern Sahara desert. (For interpretation of the references to colour in this figure legend, the reader is referred to the web version of this article.)

(Fig. 2b). In the circum-Mediterranean, Scandinavia and E-Europe get cooler in SAHARA. Temperature changes in Europe are less pronounced (less than −2 °C) than in North America. In some parts of Central Europe, temperature differences of less than −0.5 °C are even non-significant. SW-Europe and the Balkan region/Greece are more humid in the Sahara simulation (Fig. 2b). This is in contrast to drying in Central Europe in SAHARA as compared to TORT. Fig. 2a illustrates that polar regions are also cooler (up to −2 °C) and tend to be drier in the Sahara experiment (Fig. 2). It is partly possible to understand the cooling and increased sea ice cover (cf. above) in the high latitudes via the ice-albedo feedback, but this explanation is not sufficient and complete.

Fig. 4 shows the zonal average of the mean annual vertical wind of our experiments. It should be noted that the zonal averaging is performed for North Africa (from 25 °W to 60 °E) and that the vertical scale is in pressure coordinates. Negative values for the vertical wind describe rising air masses and positive values are equivalent to a downward movement. Fig. 4 illustrates that the Sahara desert noticeably affects the meridional circulation. The Sahara desert leads to a cooling in North Africa (Fig. 2a), which strengthens the descending part of the northern Hadley cell (Fig. 4) in SAHARA. The equatorial ascending branch of the Hadley cell is also stronger in SAHARA but less than the downward part. Hence, the Sahara desert intensifies the mean meridional circulation as compared to TORT because atmospheric circulation has to compensate for the reduced release of sensible and latent heat in North Africa. The cooling in North Africa (cf. Fig. 2a) is equivalent to a reduced release of sensible heat to the atmosphere in SAHARA, and more arid conditions (cf. Fig. 2c) describe a reduced source of latent heat as compared to TORT. Moreover, the intertropical convergence zone (ITCZ) is slightly farther south in SAHARA as compared to

TORT. This small shift of the ITCZ is also represented in the precipitation anomalies (Fig. 2b) in equatorial regions. Fig. 5 illustrates that the tropical easterly jet over North Africa is weaker in SAHARA. For Asia, the eastward flow intensifies in SAHARA, while contrarily westerlies are weaker into middle to higher latitudes as compared to TORT.

The Sahara desert modifies the atmospheric circulation patterns (cf. Figs. 4 and 5) in our experiment and it causes a cooling and drying in North Africa (cf. Fig. 2), which is equivalent to a reduced release of sensible and latent heat into the atmosphere in SAHARA. As a result of these modifications, the appearance of the Sahara leads to a generally weaker poleward heat transport (Fig. 6) as compared to TORT. Fig. 6 shows pronounced peaks in the differences between SAHARA and TORT, which represent the slight southward shift of the ITCZ (cf. above).

5. Discussion

In the Neogene, the North African vegetation underwent significant changes from tropical forests in the Early Miocene (Wolfe, 1985) towards the evolution of the Sahara desert in the Miocene/Pliocene (e.g., Le Houerou, 1997; Willis and McElwain, 2002). From a Late Miocene sensitivity experiment with the Earth system model of intermediate complexity Planet Simulator, we analyse the climate response to a North African desertification. By the definition of our sensitivity experiment, we do not include climate–vegetation-interaction processes. We consider only the effects of vegetation on climate.

Our Tortonian reference run is globally $+2.6$ °C warmer than a present-day control experiment. An Early Miocene model experiment demonstrates a warming of $+4$ °C as compared to a present-day control experiment (Dutton and Barron, 1997). This result agrees fairly well with our present study, considering the Early to Late Miocene general cooling trend and the usage of different climate models and model configurations.

5.1. North Africa

The Sahara experiment represents generally cooler and drier conditions as compared to the Tortonian reference experiment. A cooling and increased aridity in North Africa are consistent with the proposed self-inducing mechanisms of the Sahara (Charney, 1975; Claussen et al., 1998). For the Eemian and the mid-Holocene, model experiments also represented generally warmer and more humid conditions in a greener North Africa (Kubatzki et al., 2000; Brovkin et al., 2002). These simulations are in general agreement to our results for northern North Africa, even though climatic changes in the Quaternary modelling studies are less pronounced than in SAHARA minus TORT. Based on climate simulations for Quaternary times, it was proposed that the vegetation–albedo feedback mechanism was a major factor for triggering the African monsoon (e.g., Claussen and Gayler, 1997; de Noblet-Ducoudre et al., 2000). However, a slightly different picture was shown from Early Miocene and Pliocene model experiments. An Early Miocene model experiment focusing on the climatic effects of global vegetation changes (Early Miocene vs. present-day) demonstrated a significant cooling in Africa except that the most northern part tends to be unchanged or slightly warmer (Dutton and Barron, 1997). Similarly for the Pliocene, an AGCM study indicated cooler conditions and higher rainfall rates, if vegetation in North Africa is greener (Haywood and Valdes, 2006). These Miocene and Pliocene simulations demonstrated that evaporative cooling in North Africa is the stronger mechanism as compared to the albedo effect. With a regional climate model, Patricola and Cook (2007) emphasised that a greening of the Sahel zone led to cooling at around 6 ka BP because of a reduced cloud cover and, therefore, a lowered radiation flux. This is consistently found for the southern part of the modified area in SAHARA (cf. Figs. 2c and 7). However, the Pliocene study illustrated temperature increases and increased aridity also in the more northern part of North Africa (Haywood and Valdes, 2006), which is in contrast to our data. Temperature changes of the Early Miocene vegetation sensitivity experiment (Dutton and

Barron, 1997) support our results. In present-day simulations and in future climate change projections, temperature increases in North Africa are usually related with increased aridity (Christensen et al., 2007; Meehl et al., 2007), but the different model predictions do not show a fully coherent pattern for North Africa (Meehl et al., 2007).

Discrepancies in our study as compared to other modelling studies can be explained by the EMIC concept with its simpler parameterisation schemes (e.g., convection) as compared to complex models. Model results also depend on the boundary conditions. For instance, Claussen et al. (1998) obtained two solutions for the North African vegetation (green and desert) from an AGCM experiment forced with climatological sea surface temperatures. However, sea surface temperature variability has a significant effect on the variation of rainfall in the Sahel zone (Zeng et al., 1999). Taking this into account, there is only an intermediate equilibrium (Zeng and Neelin, 2000). Concerning the Miocene/Pliocene, other processes such as mountain uplift, the retreat of the Parathetys or the decrease of CO_2 can correspondingly lead to some differences between our study and others. This makes it even more important to consider available proxy data for the model validation.

From the latest Miocene and early Pliocene, the fossil record suggests that North Africa got more arid (Cerling et al., 1997a; Jacobs et al., 1999; Jacobs, 2004; Behrensmeyer, 2006). Hence, proxy data support the trend of decreases in annual rainfall in our Sahara experiment, even though the local response in the most northern part of Africa is weak. Rainfall strongly decreases from Turkey to India (Fig. 2b) as compared to TORT. More arid conditions in the Middle East are in agreement with the expansion of C_4-grasses and the retreat of C_3-vegetation from 8 to 6 Ma in Pakistan (Cerling et al., 1997a, 1999).

5.2. Asia

Asia tends to be generally drier in the Sahara experiment. Including a greener-than-present Sahara, sensitivity simulations for the Eemian and the mid-Holocene situation consistently represented increased aridity in Asia (Kubatzki et al., 2000; Brovkin et al., 2002). However, changes in precipitation in Central Asia are more pronounced in the Quaternary experiments than in our study. The weak response in SAHARA can be explained by amplifications due to climate–vegetation interactions in Asia, which were explicitly not included by the definition of our sensitivity scenario.

When considering Miocene/Pliocene hypsodonty data (Fig. 1), we refer to three intervals, which are the Late Tortonian (Late Bahean, 9.1 to 7.1 Ma), the Messinian (Baodean, 7.1 to 5.3 Ma) and the Early Pliocene (5.3 to 3.4 Ma). From the Late Miocene to the Early Pliocene in Central Asia, fossil mammal faunas indicate that the climate changed into drier conditions, which are also represented in the model and by other studies (e.g., Fortelius et al., 2002). In contrast, hypsodonty data suggest humid conditions in Late Bahean in south-eastern Asia, and these conditions spread to north-eastern China during the Baodean (Fig. 1a,b). Comparing the hypsodonty data (Fig. 1a,b) with the Sahara experiment (Fig. 2b), we observe large consistency between both. Hence, the stepwise pattern of spreading humid conditions in East Asia during the Late Bahean — Baodean (Fig. 1a,b) can have been linked to the successive spreading of aridity in North Africa. Of course, the uplift of the Tibetan Plateau was the dominating factor for the evolution of the Asian monsoon (e.g., Kutzbach et al., 1993; Ramstein et al., 1997; Liu and Yin, 2002; Sun and Wang, 2006). Since the Oligocene, Tibet Uplift caused increased aridity in Central Asia, while conditions in East Asia got continuously more humid. Our hypsodonty data suggest that at least during the late Miocene Tibet Uplift and the appearance of the Sahara influenced Asia in similar ways: precipitation increases in East Asia and it decreases in Central Asia. Later on in the Early Pliocene (Fig. 1c), the Central Asian aridity pattern seems well established, but only few data for East Asia were included and are hard to interpret. Before the Pliocene, the large mammal hypsodonty data seem to indicate a trend towards more humid conditions in E-/SE-Asia during 8 to 5 Ma ago (Fig. 1a,b) such as represented in SAHARA.
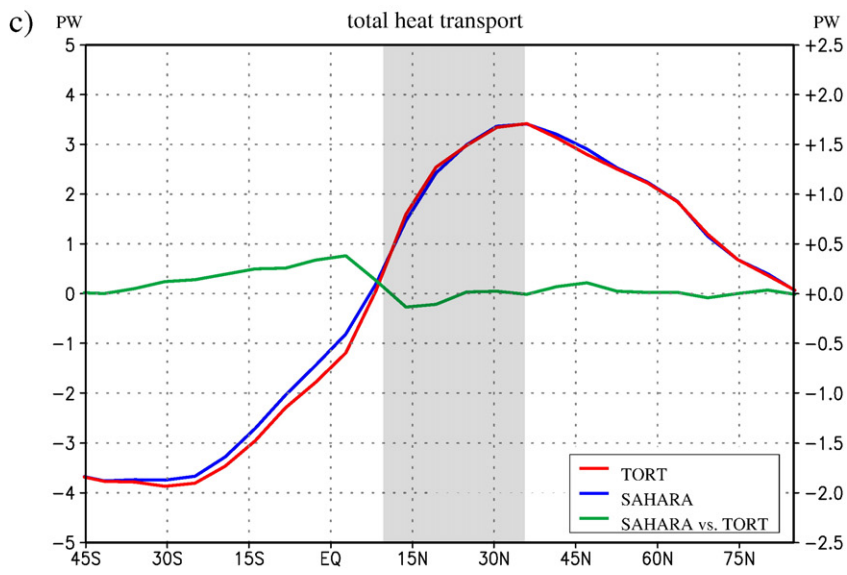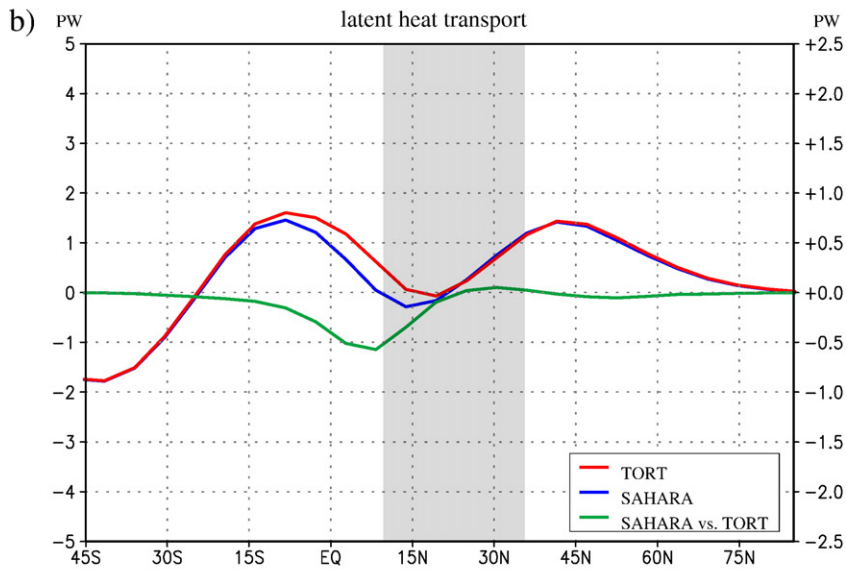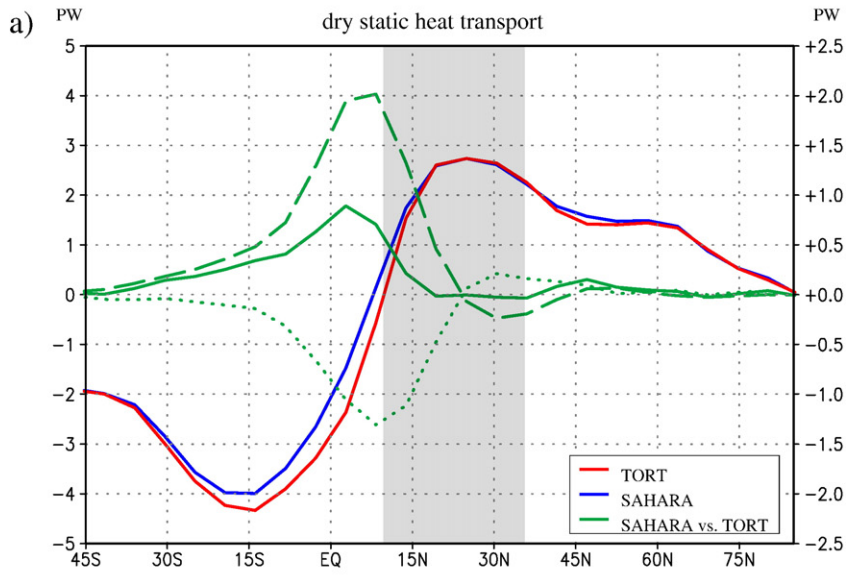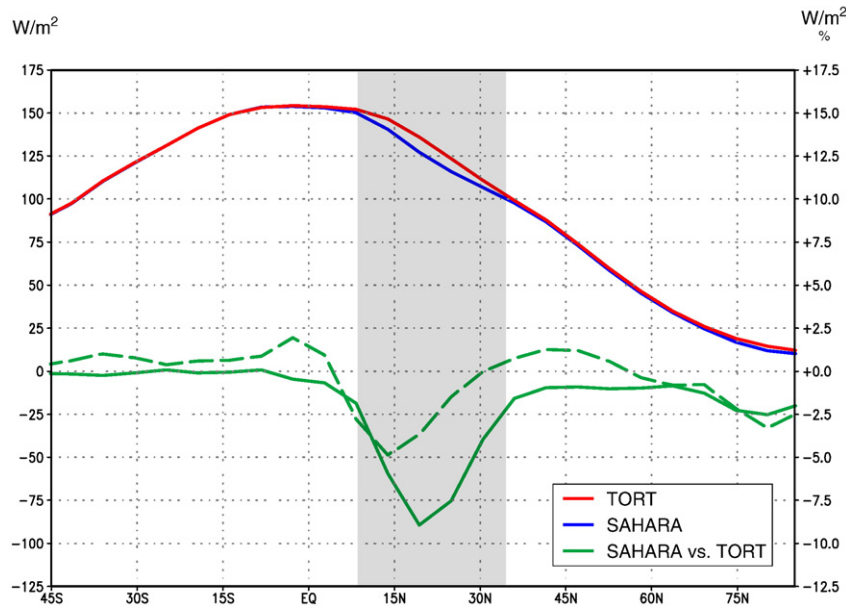
Fig. 7. The zonal and annual average net surface radiation flux density [W/m²] of TORT (red), SAHARA (blue), and the differences between SAHARA and TORT (green solid). The green dashed line illustrates the differences of the cloud cover [%] between SAHARA and TORT. Absolute values are shown against the left axis; differences refer to the right axis. The grey-shading illustrates the position of the modern Sahara desert. (For interpretation of the references to colour in this figure legend, the reader is referred to the web version of this article.)

Then, climate went over into some more arid conditions in East Asia in the Early Pliocene (Fig. 1b,c). This disagrees with the model and suggests that Tibet Uplift and the spreading of grasslands in Central Asia might have had a more relevant influence on climate than the appearance of the Sahara desert.

In SAHARA, the SE-Asian monsoon slightly intensifies as compared to TORT. The onset of the Asian monsoon was at around 20 Ma (Sun and Wang, 2006), but due to the low elevation of the Tibet Plateau it was generally weak as compared to today (Ding et al., 1999; Sun and Wang, 2006). In the latest Miocene to early Pliocene, the Asian monsoon intensified (Sun and Wang, 2006) and got even stronger than in the Holocene (Ding et al., 1999, 2001). The explanation of a strong monsoon at that time is not fully clear as Tibet uplift still continued (Ding et al., 1999). Our results suggest that the evolution of the Sahara contributed to a strengthened SE-Asian monsoon, even though Tibet was still low. In Asia, the response to the appearance of the Sahara is weak in our study. Therefore, the results should not be over-estimated and regarding the evolution of the Asian monsoon due to Tibet uplift in the Cenozoic we refer the reader to other studies (e.g. Ramstein et al., 1997; Fluteau et al., 1999; Kutzbach and Behling, 2004).

5.3. Europe

SW-Europe is cooler and tends to be slightly more humid in the Sahara simulation. For the W-Mediterranean region (Spain/North Africa), however, palaeobotanical data indicate some warmer and drier conditions in the Early Pliocene than in the Tortonian (Fauquette et al., 2007). Moreover, there occurred a transition from temperate-humid into subtropical-dry conditions in NE-Spain in the Late Miocene (Alonzo-Zarza and Calvo, 2000). The small and large mammal record of central-eastern Spain also indicate increasingly dry conditions from the late Miocene into the Pliocene (Fortelius et al., 2002; Eronen and Rook, 2004; Fortelius et al., 2006; van Dam, 2006). These findings disagree with our model results, but can be explained by other processes such as the intensification of the thermohaline circulation in the North Atlantic

(e.g., Mikolajewicz and Crowley, 1997), which were probably more important for the SW-European climate evolution.

For France, SAHARA demonstrates no significant cooling as compared to TORT. This is consistent to Montuire et al. (2006) proposing that there were no major environmental changes between the Late Miocene and the Pliocene in E-Spain and S-France. Palaeobotanical evidences from SW-France also support these findings (Fauquette et al., 2007). However, a flora from the Massif Central indicated a cooling trend between 7 and 5.5 Ma (Roiron., 1991). This agrees with the trend of our sensitivity study, even though tectonic uplift played an important role for climate evolution in Europe (e.g., Spiegel et al., 2001; Bruch et al., 2006).

E-/SE-Europe is cooler in SAHARA than in TORT. Palaeobotanical evidences consistently show that Hungary became slightly cooler in the Late Miocene and only minor environmental changes occurred from the Sarmatian to the Pliocene (Hably, 2003). In the Balkan region/Greece, precipitation increases in the Sahara experiment. This is in contrast to the overall European drying trend as compared to TORT, but plant megafossils for this region support a cooling trend and slightly more humid conditions from the Late Miocene to the Pliocene (Kovar-Eder et al., 2006). According to fossil mammals evidence, humid conditions at that time were prevalent just north of the Alps and in the Pannonian Basin (Fortelius et al., 2002; Eronen and Rook, 2004; Fortelius et al., 2006). For the Pannonian Basin, the sensitivity experiment is consistent to proxy data. More humid conditions north of the Alps cannot be seen in SAHARA, but can be explained by e.g. tectonic changes and their impact on climate not represented in SAHARA. Also, the evolution of the North Atlantic thermohaline circulation at that time had a relevant influence on the European climate (e.g., Mikolajewicz and Crowley, 1997; Haywood et al., 2000b).

5.4. North America

In North America, the desertification of North Africa leads to a cooling. The fossil record consistently indicates that the Great Plains

Fig. 6. The vertically and zonally integrated time averages of a) the dry static, b) the latent, and c) the total heat transport of TORT (red), SAHARA (blue), and the differences between SAHARA and TORT (green). Units are PW (10^{15} W). Absolute values are shown against the left axis; differences refer to the right axis. In a) differences between SAHARA and TORT are split up into the sensible (dotted) and potential (dashed) heat transport. The grey-shading in a) to c) illustrates the position of the modern Sahara desert. (For interpretation of the references to colour in this figure legend, the reader is referred to the web version of this article.)

experienced a cooling from 6.4 Ma to 2.5 Ma (Fox and Koch, 2004). Fossil crocodilians became more restricted to southern parts of North America from the Miocene to the Pliocene (Markwick, 1998), where the cooling in SAHARA minus TORT is less pronounced. This supports our results. Based on SAHARA, the long-term cooling trend in North America is partly related to the introduction of the Sahara.

5.5. Atmospheric circulation

From our sensitivity experiment, we observe that the appearance of the Sahara leads to a weakening of the tropical easterly jet and the westerlies. Similarly, Quaternary sensitivity studies with global atmospheric general circulation models demonstrated that the tropical easterly jet and westerlies are weaker in the case of a deserted North Africa as compared to a greener-than-present Sahara (Kubatzki and Claussen, 1998; Kubatzki et al., 2000). In contrast, Cook (1999) emphasised that the formation of the tropical easterly jet is linked to solar forcing and aridity in North Africa during the summer season. Using a regional climate model, Patricola and Cook (2007) accordingly demonstrated that an increase in precipitation due to a greener-than-present North Africa at around 6 ka does not allow for the formation of the easterly jet. This contradicts our results as well as others (e.g., Kubatzki and Claussen, 1998), but can be explained by the coarse spatial resolution of global models as compared to regional models and by simplified representations of physical processes in our EMIC as compared to complex models.

The intensification of the meridional circulation in the lower latitudes (cf. above) increases the southward transport of sensible heat towards equatorial regions as compared to TORT (Fig. 6a). This explains the warming south of the Sahara (cf. Fig. 2a). For the Southern Hemisphere, the sensible heat flux in SAHARA indicates a reduced transport towards the equatorial zone. The decrease of the latent heat transport (Fig. 6b) in SAHARA indicates an increased transport of moisture towards the equator. This leads to enhanced rainfall as compared to the Tortonian reference experiment (cf. Fig. 2b). Both the sensible and latent heat fluxes decrease in the Sahara experiment. For the part north of the zero-crossing of the graphs, this would mean a less efficient poleward (i.e., northward) heat transport in SAHARA. Contrarily for the southern part, it would describe a more efficient poleward (i.e., southward) heat transport than in TORT. This is, however, not shown from the total atmospheric heat transport (Fig. 6c) because the potential energy transport is largely modified (Fig. 6a) in SAHARA as compared to TORT. On the one hand, the increased potential energy flux is equivalent to a slightly more efficient northward transport in the Northern Hemisphere in SAHARA. On the other hand, the increased potential heat flux in the Southern Hemisphere describes a less efficient southward transport than in the Tortonian reference run. Hence, the atmospheric poleward heat transport in the low latitudes is generally less efficient in SAHARA (Fig. 6c).

The atmospheric heat flux in the northern mid- to high latitudes is not much affected by the introduction of the Sahara. This seems to be enigmatic because obviously the Sahara contributes to a cooling of higher latitudes (Fig. 2a). Fig. 7 illustrates the radiation budget at the Earth's surface and the total cloud cover between SAHARA and TORT. Focusing on the high northern latitudes, the surface radiation energy budget in SAHARA is reduced. This correlates with a lower cloud cover than in TORT. From the mid- to high latitudes of the Northern Hemisphere, the northward latent heat flux (Fig. 6b) in SAHARA is only slightly less efficient than in TORT. However, this small reduction is enough so that some little more moisture remains in the mid-latitudes (slightly increasing cloud cover and precipitation, cf. Fig. 2b) and a little less moisture reaches polar regions. Correspondingly, the cloud cover in high latitudes is reduced as compared to TORT and less radiation energy can be trapped in the Earth system (Fig. 7). As a result of the slightly reduced northward latent heat transport, the cloud-radiation feedback process leads to the cooling of the high latitudes in

the Sahara experiment. This cooling in SAHARA is slightly amplified by the sea ice-albedo feedback mechanism (cf. above).

The Sahara experiment represents cooler conditions in the higher latitudes as compared to the Tortonian reference experiment. In the late Cenozoic, global cooling was most pronounced in middle to high latitudes, which increased the meridional temperature gradient (e.g., Wolfe, 1994a,b; Bruch et al., 2004; Mosbrugger et al., 2005; Fauquette et al., 2007). The appearance of the Sahara desert in the Miocene/Pliocene can contribute to a less efficient northward heat transport in the atmosphere. In particular, a small reduction of the northward latent heat flux in the Sahara experiment is important to induce a cloud-radiation feedback process in higher latitudes, which leads to a cooling of polar regions. For this reason, the introduction of the Sahara desert provides a mechanism to partly explain the cooling and drying of higher latitudes in the late Cenozoic.

6. Conclusions

Our sensitivity experiment demonstrates that the North African vegetation change from grassland to desert significantly changes the Miocene climate on the Northern Hemisphere. The introduction of the modern Sahara desert leads to a general cooling (albedo effect) and to increased aridity (reduced evapotranspiration) in the most arid part of Africa. In contrast to the cooler north, the more humid southern part of the Sahara and Central Africa get warmer because the reduced evaporative cooling dominates over the albedo effect. Thus, the climate response to the appearance of the Sahara desert strongly depends on the hydrological regime. In our Sahara simulation, the meridional circulation intensifies and the tropical easterly jet is slightly displaced towards the south over North Africa. Furthermore, we observe teleconnection patterns related to the North African desertification in our Late Miocene sensitivity experiment: Central Asia is cooler and more arid, and North America gets cooler. As compared to hypsodonty data for Central Asia, the model represents a too weakly increased aridity due to the Sahara desert. This might be due to the excluded vegetation changes in Central Asia as well as the further uplift of the Tibetan Plateau.

Overall, the North African aridification in the low latitudes during the Miocene contributes to a cooling of the middle and high latitudes in the Miocene/Pliocene. Thus, vegetation changes (which are themselves caused by other factors such as mountain uplift) towards more open landscapes in subtropical latitudes provide a mechanism to partly explain the Late Cenozoic climate cooling. Finally, we observe that the North African aridification is related with higher rainfalls in E-/SE-Asia. Hence, the appearance of the Sahara can partly explain why the Asian monsoon in the Pliocene can have been stronger than in the Holocene even though the Tibet Plateau was still low.

Vegetation changes in the Miocene were not necessarily the original causes of climatic changes, but they contributed or even amplified them. Such as represented in our Late Miocene sensitivity experiment, the opening of the landscapes and the desertification in tropical/subtropical latitudes can have altered climatic conditions in other regions (teleconnections). When exceeding critical thresholds e.g. in mid-latitudes, further feedbacks such as the expansion of grasslands in Central Asia can be induced or amplified. Then, this again can have led or contributed to a cooling in higher latitudes. The appearance of the Sahara desert is not the very beginning in explaining the Cenozoic cooling, but it is one piece in the puzzle. The climate response represented in the model should not be over-interpreted. It is, however, encouraging that the simulation demonstrates largely consistent patterns as compared to the fossil record.

From our sensitivity experiment, we observe that in North Africa the climate response to the introduction of the Sahara desert is more pronounced than in Quaternary climate modelling studies (e.g., Kubatzki et al., 2000; Brovkin et al., 2002). On the one hand, this indicates that climate sensitivity can be different in a hothouse

(Miocene) as compared to an icehouse (Quaternary) situation. On the other hand, the different models can cause slightly different results such as reported for future climate change scenarios (e.g., Meehl et al., 2007). There are also some uncertainties in our set of Late Miocene boundary conditions (e.g., ocean heat transport). Further experiments should test how robust our results are with respect to modified boundary conditions. Last but not least, vegetation is a prescribed parameter in our study and further experiments could use dynamic vegetation modules to get deeper knowledge about climate–vegetation feedback mechanisms.

Acknowledgements

References

Alonzo-Zarza, A.M., Calvo, J.P., 2000. Palustrine sedimentation in an episodically subsiding basin: the Miocene of the northern Teruel Graben (Spain). Palaeogeogr. Palaeoclim. Palaeoecol. 160, 1–21.

Behrensmeyer, A.K., 2006. Climate change and human evolution. Science 311, 476–478.

Bice, K.L., Scotese, C.R., Seidov, D., Barron, E.J., 2000. Quantifying the role of geographic change in Cenozoic ocean heat transport using uncoupled atmosphere and ocean models. Palaeogeogr. Palaeoclim. Palaeoecol. 161, 295–310.

Brovkin, V., Bendtsen, J., Claussen, M., Ganopolski, A., Kubatzki, C., Petoukhov, V., Andreev, A., 2002. Carbon cycle, vegetation, and climate dynamics in the Holocene: experiments with the CLIMBER-2 model. Glob. Biogeochem. Cycles 16 (4), 1139.

Bruch, A.A., Utescher, T., Alcalde Olivares, C., Dolakova, N., Mosbrugger, V., 2004. Middle and Late Miocene spatial temperature patterns and gradients in Central Europe — preliminary results based on paleobotanical climate reconstructions. Cour. Forsch. Inst. Senckenb. 249, 15–27.

Bruch, A.A., Utescher, T., Mosbrugger, V., Gabrielyan, I., Ivanov, D.A., 2006. Late Miocene climate in the circum-Alpine realm—a quantitative analysis of terrestrial paleo-floras. Palaeogeogr. Palaeoclim. Palaeoecol. 238, 270–280.

Cerling, T.E., Harris, J.M., MacFadden, B.J., Leakey, M.G., Quade, J., Eisenmann, V., Ehleringer, J.R., 1997a. Global vegetation change through the Miocene/Pliocene boundary. Nature 389, 153–159.

Cerling, T.E., Quade, J., Ambrose, S.H., Sikes, N.E., 1997b. Fossil soils, grasses, and carbon isotopes from Fort Ternan, Kenya: grassland or woodland? J. Hum. Evol. 21, 295–306.

Cerling, T.E., Harris, J.M., Leakey, M.G., 1999. Browsing and grazing in elephants: the isotope record of modern and fossil proboscideans. Oecologia 120, 364–374.

Charney, J.G., 1975. Dynamics of deserts and drought in the Sahel. Q. J. R. Meteorol. Soc. 101, 193–202.

Claussen, M., Gayler, V., 1997. The greening of Sahara during the mid-Holocene: results of an interactive atmosphere–biome model. Glob. Ecol. Biogeogr. Lett. 6, 369–377.

Claussen, M., Brovkin, V., Ganopolski, A., Kubatzki, C., Petoukhov, V., 1998. Modeling global terrestrial vegetation–climate interaction. Philos. Trans. R. Soc. Lond. B 353, 53–63.

Claussen, M., Brovkin, V., Ganopolski, A., Kubatzki, C., Petoukhov, V., 2003. Climate change in Northern Africa: the past is not the future. Clim. Change 57, 99–118.

Christensen, J.H., Hewitson, B., Busuioc, A., Chen, A., Gao, X., Held, I., Jones, R., Kolli, R.K., Kwon, W.-T., Laprise, R., Magaña Rueda, V., Mearns, L., Menéndez, C.G., Räisänen, J., Rinke, A., Sarr, A., Whetton, P., 2007. Regional climate projections. In: Solomon, S., Qin, D., Manning, M., Chen, Z., Marquis, M., Averyt, K.B., Tignor, M., Miller, H.L. (Eds.), Climate Change 2007: The Physical Science Basis. Contribution of Working Group I to the Fourth Assessment Report of the Intergovernmental Panel on Climate Change. Cambridge University Press, Cambridge, pp. 847–940.

Cook, K.H., 1999. Generation of the African easterly jet and its role in determining West African precipitation. J. Climate 12, 1165–1184.

Damuth, J., Fortelius, M., 2001. Reconstructing mean annual precipitation, based on mammalian dental morphology and local species richness. In: Agusti, J., Oms, O. (Eds.), EEDEN Plenary Workshop on Late Miocene to early Pliocene Environments and Ecosystems, EEDEN Programme. European Science Foundation, Sabadell, Spain, pp. 23–24.

de Noblet-Ducoudre, N., Claussen, M., Prentice, C., 2000. Mid-Holocene greening of the Sahara: first results of the GAIM 6000 year BP experiment with two asynchronously coupled atmosphere/biome models. Clim. Dyn. 16 (9), 643–659.

Ding, Z.L., Xiong, S.F., Sun, J.M., Yang, S.L., Gu, Z.Y., Liu, T.S., 1999. Pedostratigraphy and paleomagnetism of a approximately 7.0 Ma eolian loess-red clay sequence at Lingtai, Loess Plateau, north-central China and the implications for paleomonsoon evolution. Palaeogeogr. Palaeoclim. Palaeoecol. 152, 49–66.

Ding, Z.L., Yang, S.L., Sun, J.M., Liu, T.S., 2001. Iron geochemistry of loess and red clay deposits in the Chinese Loess Plateau and implications for long-term Asian monsoon evolution in the last 7.0 Ma. Earth Planet. Sci. Lett. 185, 99–109.

Dutton, J.F., Barron, E.J., 1997. Miocene to present vegetation changes: a possible piece of the Cenozoic puzzle. Geology 25 (1), 39–41.

Eronen, J.T., Rook, L., 2004. The Mio-Pliocene European primate fossil record: dynamics and habitat tracking. J. Hum. Evol. 47, 323–341.

Fauquette, S., Suc, J.-P., Jiminez-Moreno, G., Favre, E., Jost, A., Micheels, A., Bachiri-Taoifiq, N., Bertini, A., Clet-Pellegrin, N., Diniz, F., Farjanel, G., Feddi, N., Zheng, Z., 2007. Latitudinal climatic gradients in Western European and Mediterranean regions from the Mid-Miocene (~15 Ma) to the Mid-Pliocene (~3.6 Ma) as quantified from pollen data. In: Williams, M., Haywood, A.M., Gregory, F.J., Schmidt, D.N. (Eds.), Deep-Time Perspectives on Climate Change: Marrying the Signal from Computer Models and Biological Proxies. The Micropalaeontological Society, Special Publications. The Geological Society, London, pp. 481–502.

Fluteau, F., Ramstein, G., Besse, J., 1999. Simulating the evolution of the Asian and African monsoons during the past 30 Myr using an atmospheric general circulation model. J. Geophys. Res. 104, 11995–12018.

Fortelius, M., Eronen, J.T., Jernvall, J., Liu, L., Pushkina, D., Rinne, J., Tesakov, A., Vislobokova, I.N., Zhang, Z., Zhou, L., 2002. Fossil mammals resolve regional patterns of Eurasian climate change during 20 million years. Evol. Ecol. Res. 4, 1005–1016.

Fortelius, M., Eronen, J.T., Liu, L., Pushkina, D., Tesakov, A., Vislobokova, I.A., Zhang, Z., 2003. Continental-scale hypsodonty patterns, climatic paleobiogeography, and dispersal of Eurasian Neogene large mammal herbivores. In: Reumer, J.W.F., Wessels, W. (Eds.), Distribution and Migration of Tertiary Mammals in Eurasia. A volume in honour of Hans de Bruijn, Deinsea, vol. 10, pp. 1–11. Utrecht, The Netherlands.

Fortelius, M., Eronen, J., Liu, L., Pushkina, D., Tesakov, A., Vislobokova, I., Zhang, Z., 2006. Late Miocene and Pliocene large land mammals and climatic changes in Eurasia. Palaeogeogr. Palaeoecol. 238, 219–227.

Fox, D.L., Koch, P.L., 2004. Carbon and oxygen isotopic variability in Neogene paleosol carbonates: constraints on the evolution of the C_4-grasslands of the Great Plains, USA. Palaeogeogr. Palaeoclim. Palaeoecol. 207, 305–329.

Fraedrich, K., Kirk, E., Lunkeit, F., 1998. PUMA: Portable University Model of the atmosphere. DKRZ Technical Report, 16, Max-Planck-Institut für Meteorologie, 24 pp. http://www.mad.zmaw.de/fileadmin/extern/documents/reports/ReportNo.16.pdf.

Fraedrich, K., Jansen, H., Kirk, E., Luksch, U., Lunkeit, F., 2005a. The planet simulator: towards a user friendly model. Meteorol. Z. 14, 299–304. http://www.mi.uni-hamburg.de/fileadmin/files/forschung/theomet/planet_simulator/downloads/plasim_mz_1.pdf.

Fraedrich, K., Jansen, H., Kirk, E., Lunkeit, F., 2005b. The planet simulator: green planet and desert world. Meteorol. Z. 14, 305–314. http://www.mi.uni-hamburg.de/fileadmin/files/forschung/theomet/planet_simulator/downloads/plasim_mz_2.pdf.

Frisius, T., Lunkeit, F., Fraedrich, K., James, I.A., 1998. Storm-track organization and variability in a simplified atmospheric global circulation model. Q. J. R. Meteorol. Soc. 124, 1019–1043.

Grosfeld, K., Lohmann, G., Rimbu, N., Fraedrich, K., Lunkeit, F., 2007. Atmospheric multidecadal variations in the North Atlantic realm: proxy data, observations, and atmospheric circulation model studies. Clim. Past 3, 39–50.

Hably, L., 2003. Late Neogen vegetation and climate reconstruction in Hungary. Acta Univ. Carol., Geol. 46 (4), 85–90.

Haywood, A.M., Valdes, P.J., 2006. Vegetation cover in a warmer world simulated using a dynamic global vegetation model for the Mid-Pliocene. Palaeogeogr. Palaeoclim. Palaeoecol. 237, 412–427.

Haywood, A.M., Sellwood, B.W., Valdes, P.J., 2000a. Regional warming: Pliocene (ca. 3 Ma) paleoclimate of Europe and the Mediterranean. Geology 28, 1063–1066.

Haywood, A.M., Valdes, P.J., Sellwood, B.W., 2000b. Global scale paleoclimate reconstruction of the middle Pliocene climate using the UKMO GCM: initial results. Glob. Planet. Change 25, 239–256.

Jacobs, B.F., 2004. Paleobotanical studies from tropical Africa: relevance to the evolution of forest, woodland and savannah biomes. Philos. Trans. R. Soc. Lond. B 359, 1573–1583.

Jacobs, B.F., Kingston, J.D., Jacobs, L.L., 1999. The origin of grass-dominated ecosystems. Ann. Mo. Bot. Gard. 86 (2), 590–643.

Jimenez-Moreno, G., Rodriguez-Tovar, F.J., Pardo-Iguzquiza, E., Fauquette, S., Suc, J.-P., Muller, P., 2005. High-resolution palynological analysis in late early–middle Miocene Tengelic-2 core from the Pannonian Basin, Hungary: climatic changes, astronomical forcing and eustatic fluctuations in the Central Paratethys. Palaeogeogr. Palaeoclim. Palaeoecol. 216, 73–97.

Junge, M.M., Lunkeit, F., Fraedrich, K., Gayler, V., Blender, R., Luksch, U., 2005. A world without Greenland: impacts on northern hemisphere circulation in low and high resolution models. Clim. Dyn. 24, 297–307.

Kleidon, A., Fraedrich, K., Low, C., 2007. Multiple steady-states in the terrestrial atmosphere–biosphere system: a result of a discrete vegetation classification? Biogeosci. Discuss. 4, 687–705.

Kovar-Eder, J., Kvacek, Z., Martinetto, E., Roiron, P., 2006. Late Miocene to Early Pliocene vegetation of southern Europe (7–4 Ma) as reflected in the megafossil plant record. Palaeogeogr. Palaeoclim. Palaeoecol. 238, 321–339.

Kubatzki, C., Claussen, M., 1998. Simulation of the global bio-geophysical interactions during the Last Glacial Maximum. Clim. Dyn. 14, 461–471.

Kubatzki, C., Montoya, M., Rahmsdorf, S., Ganopolski, A., Claussen, M., 2000. Comparison of the last interglacial climate simulated by a coupled global model of intermediate complexity and an AOGCM. Clim. Dyn. 16, 799–814.

Kürschner, W.M., van der Burgh, J., Visscher, H., Dilcher, D., 1996. Oak leaves as biosensor of late Neogene and early Pleistocene paleoatmospheric CO_2 concentrations. Mar. Micropaleontol. 27, 299–312.

Kutzbach, J.E., Behling, P., 2004. Comparison of simulated changes of climate in Asia for two scenarios: Early Miocene to present, and present to future enhanced greenhouse. Glob. Planet. Change 41, 157–165.

Kutzbach, J.E., Prell, W., Ruddiman, W.F., 1993. Sensitivity of Eurasian climate to surface uplift of the Tibetan Plateau. J. Geol. 101, 177–190.

Le Houerou, H.N., 1997. Climate, flora and fauna changes in the Sahara over the past 500 million years. J. Arid Environ. 37, 619–647.

Liu, X., Yin, Z.-Y., 2002. Sensitivity of East Asian monsoon climate to the uplift of the Tibetan Plateau. Palaeogeogr. Palaeoclim. Palaeoecol. 183, 223–245.

MacFadden, B.J., 2005. Terrestrial mammalian herbivore response to declining levels of atmospheric CO_2 during the Cenozoic: evidence from North American fossil horses (family Equidae). In: Ehleringer, J.R., Cerling, T.E., Dearing, M.D. (Eds.), A History of Atmospheric CO_2 and Its Effects on Plants, Animals, and Ecosystems. Ecological Studies, vol. 177, pp. 273–292.

Markwick, P.J., 1998. Fossil crocodilians as indicator of late Cretaceous and Cenozoic climates: implications for using paleontological data in reconstructing paleoclimate. Palaeogeogr. Palaeoclim. Palaeoecol. 137, 205–271.

Meehl, G.A., Stocker, T.F., Collins, W.D., Friedlingstein, P., Gaye, A.T., Gregory, J.M., Kitoh, A., Knutti, R., Murphy, J.M., Noda, A., Raper, S.C.B., Watterson, I.G., Weaver, A.J., Zhao, Z.-C., 2007. Regional climate projections. In: Solomon, S., Qin, D., Manning, M., Chen, Z., Marquis, M., Averyt, K.B., Tignor, M., Miller, H.L. (Eds.), Climate Change 2007: The Physical Science Basis. Contribution of Working Group I to the Fourth Assessment Report of the Intergovernmental Panel on Climate Change. Cambridge University Press, Cambridge, pp. 747–845.

Micheels, A., Montenari, M., 2008. A snowball Earth versus a slushball Earth: results from Neoproterozoic climate modelling sensitivity experiments. Geosphere 4 (2), 401–410.

Micheels, A., Bruch, A.A., Mosbrugger, V., Uhl, D., Utescher, T., 2006. Simulating climatic effects of palaeovegetation changes in the Late Miocene using different climate models. 7th European Palaeobotany–Palynology Conference, Prague, p. 93.

Micheels, A., Bruch, A.A., Uhl, D., Utescher, T., Mosbrugger, V., 2007. A Late Miocene climate model simulation with ECHAM4/ML and its quantitative validation with terrestrial proxy data. Palaeogeogr. Palaeoclim. Palaeoecol. 253, 267–286.

Micheels, A., Bruch, A., Mosbrugger, V., submitted for publication. Miocene climate modelling sensitivity experiments for different CO_2 concentrations. Palaeontologica Electronica, in revision.

Mikolajewicz, U., Crowley, T.J., 1997. Response of a coupled ocean/energy balance model to restricted flow through the central American isthmus. Paleoceanography 12 (3), 429–441.

Molnar, P., 2005. Mio-Pliocene growth of the Tibetan Plateau and evolution of East Asian climate. Paleontol. Electron. 8 (1), 1–23. http://paleo-electronica.org/paleo/2005_1/molnar2/issue1_05.htm.

Montuire, S., Maridet, O., Legendre, S., 2006. Late Miocene–Early Pliocene temperature estimates in Europe using rodents. Palaeogeogr. Palaeoecol. 238, 247–262.

Mosbrugger, V., Utescher, T., Dilcher, D.L., 2005. Cenozoic continental climatic evolution of Central Europe. Proc. Natl. Acad. Sci. 102, 14964–14969.

Pagani, M., Zachos, J.C., Freeman, K.H., Tipple, B., Bohaty, S., 2005. Marked decline in atmospheric carbon dioxide concentrations during the Paleogene. Science 309, 600–603.

Patricola, C.M., Cook, K.H., 2007. Dynamics of the West African monsoon under mid-Holocene precessional forcing: regional climate model simulations. J. Climate 20, 694–716.

Pearson, P.N., Palmer, M.R., 2000. Atmospheric carbon dioxide concentrations over the past 60 million years. Nature 406, 695–699.

Pickford, M., 2000. Crocodiles from the Beglia Formation, Middle/Late Miocene Boundary, Tunisia, and their significance for Saharan palaeoclimatology. Ann. Paleontol. 86 (1), 59–67.

Popov, S.V., Rögl, F., Rozanov, A.Y., Steininger, F.F., Shcherba, I.G., Kovac, M., 2004. Lithological-paleogeographic maps of Paratethys. 10 maps Late Eocene to Pliocene. Cour. Forsch. Inst. Senckenb. 250, 1–46.

Pott, R., 1995. The origin of grassland plant species and grassland communities in Central Europe. Fitosociologia 29, 7–32.

Ramstein, G., Fluteau, F., Besse, J., Joussaume, S., 1997. Effect of orogeny, plate motion and land–sea distribution on Eurasian climate change over past 30 million years. Nature 386, 788–795.

Retallack, G., 2001. Cenozoic expansion of grasslands and climatic cooling. J. Geol. 109, 407–426.

Roeckner, E., Brokopf, R., Esch, M., Giorgetta, M., Hagemann, S., Kornblueh, L., Manzini, E., Schlese, U., Schulzweida, U., 2006. Sensitivity of simulated climate to horizontal and vertical resolution in the ECHAM5 atmosphere model. J. Climate 19, 3771–3791.

Roiron, P., 1991. The upper Miocene macroflora from diatomites of Murat (Cantal, France) paleoclimatic implications. Paleontogr., Abt. B 223, 169–203.

Romanova, V., Lohmann, G., Grosfeld, K., 2006. Effect of land albedo, CO_2, orography, and oceanic heat transport on extreme climates. Clim. Past 2, 31–42.

Ruddiman, W.F., Kutzbach, J.E., Prentice, I.C., 1997. Testing the climatic effects of orography and CO_2 with general circulation and biome models. In: Ruddiman, W.F. (Ed.), Tectonic Uplift and Climate Change. Plenum, New York, pp. 203–235.

Schuster, M., Duringer, P., Ghienne, J.-F., Vignaud, P., Mackaye, H.T., Likius, A., Brunet, M., 2006. The age of the Sahara. Science 311, 821.

Sepulchre, P., Ramstein, G., Fluteau, F., Schuster, M., Tierclin, J.-J., Brunet, M., 2006. Tectonic uplift and Eastern Africa aridification. Science 313, 1419–1423.

Spicer, R.A., Harris, N.B.W., Widdowson, M., Herman, A.B., Guo, S., Valdes, P.J., Wolfe, J.A., Kelley, S.P., 2003. Constant elevation of southern Tibet over the past 15 million years. Nature 421, 622–624.

Spiegel, C., Kuhlemann, J., Dunkl, I., Frisch, W., 2001. Paleogeography and catchment evolution in a mobile orogenic belt: the Central Alps in Oligo-Miocene times. Tectonophysics 341 (1–4), 33–47.

Steininger, F.F., 1999. Chronostratigraphy, geochronology and biochronology of the Miocene European Land Mammal Mega-Zones (ELMMZ) and the Miocene mammal-zones. In: Rössner, G.E., Heissig, K. (Eds.), The Miocene Land Mammals of Europe. Verlag Dr. Friedrich Pfeil, pp. 9–24.

Steininger, F.F., Berggren, W.A., Kent, D.V., Bernor, R.H., Sen, S., Agusti, J., 1996. Circum-Mediterranean Neogene (Miocene–Pliocene) marine-continental chronologic correlations of European mammal units. In: Bernor, R.L., Fahlbusch, V., Mittmann, H.-V. (Eds.), The Evolution of Western Eurasian Neogene Mammal Faunas. Columbia University Press, New York, pp. 7–46.

Steppuhn, A., Micheels, A., Geiger, G., Mosbrugger, V., 2006. Reconstructing the Late Miocene climate and oceanic heat flux using the AGCM ECHAM4 coupled to a mixed-layer ocean model with adjusted flux correction. Palaeogeogr. Palaeoclim. Palaeoecol. 238, 399–423.

Steppuhn, A., Micheels, A., Bruch, A.A., Uhl, D., Utescher, T., Mosbrugger, V., 2007. The sensitivity of ECHAM4/ML to a double CO_2 scenario for the Late Miocene and the comparison to terrestrial proxy data. Global and Planetary Change 57, 189–212.

Strömberg, C.A.E., 2002. The origin and spread of grass-dominated ecosystems in the Late Tertiary of North America: preliminary results concerning the evolution of hypsodonty. Palaeogeogr. Palaeoclim. Palaeoecol. 177, 59–75.

Strömberg, C.A.E., 2004. Using phytolith assemblages to reconstruct the origin and spread of grass-dominated habitats in the Great Plains during the late Eocene to early Miocene. Palaeogeogr. Palaeoclim. Palaeoecol. 207, 239–275.

Sun, X., Wang, P., 2006. How old is the Asian monsoon system? — paleobotanical records from China. Palaeogeogr. Palaeoclim. Palaeoecol. 222, 181–222.

van Dam, J., 2006. Geographic and temporal patterns in the late Neogene (12–3 Ma) aridification of Europe: the use of small mammals as paleoprecipitation proxies. Palaeogeogr. Palaeoecol. 238, 190–218.

Vignaud, P., Duringer, P., Mackaye, H.T., Likius, A., Blondel, C., Boisserie, J.-R., de Bonis, L., Eisenmann, V., Etienne, M.E., Geraads, D., Guy, F., Lehmann, T., Lihoreau, F., Lopez-Martinez, N., Mourer-Chauvireq, C., Otero, O., Rage, J.-C., Schuster, M., Viriot, L., Zazzo, A., Brunet, M., 2002. Geology and paleontology of the Upper Miocene Toros–Menalla hominid locality, Chad. Nature 418, 152–155.

Willis, K.J., McElwain, J.C., 2002. The Evolution of Plants. Oxford Univ. Press, Oxford. 378 pp.

Wolfe, J.A., 1985. Distribution of major vegetational types during the Tertiary. In: Sundquist, E.T., Broecker, W.S. (Eds.), The Carbon Cycle and Atmospheric CO_2 Natural Variations Archean to Present. American Geophysical Union, Washington D.C, pp. 357–375.

Wolfe, J.A., 1994a. Tertiary climatic changes at middle latitudes of western North America. Palaeogeogr. Palaeoclim. Palaeoecol. 108, 195–205.

Wolfe, J.A., 1994b. An analysis of Neogene climates in Beringia. Palaeogeogr. Palaeoclim. Palaeoecol. 108, 207–216.

Zachos, J., Pagani, M., Sloan, L., Thomas, E., Billups, K., 2001. Trends, rhythms, and aberrations in global climate 65 Ma to present. Science 292, 686–693.

Zeng, N., Neelin, J.D., 2000. The role of vegetation–climate interaction and interannual variability in shaping the African savanna. J. Climate 13, 2665–2670.

Zeng, N., Neelin, J.D., Lau, K.-M., Tucker, C.J., 1999. Enhancement of interdecadal climate variability in the Sahel by vegetation interaction. Science 286, 1537–1540.

Zhang, Z.Q., Liu, L., 2005. The Late Neogene mammal biochronology in the Loess Plateau, China. Ann. Paleontol. 91, 257–266.